Available online at www.sciencedirect.com
ScienceDirect
Journal of Power Sources 176 (2008) 369–372
JOURNAL OF POWER SOURCES
www.elsevier.com/locate/jpowsour

Short communication

Novel carbon nanofiber-cobalt oxide composites for lithium storage with large capacity and high reversibility

Wen-Li Yao, Jiu-Lin Wang, Jun Yang *, Guo-Dong Du

Department of Chemical Engineering, Shanghai Jiao Tong University, Shanghai 200240, China

Received 28 August 2007; received in revised form 17 October 2007; accepted 23 October 2007
Available online 30 October 2007

Abstract

Carbon nanofiber (CNF)-Co_3O_4 composites were prepared by the calcination of CNF-$Co(OH)_2$ composite precursors under argon atmosphere. SEM and TEM observations revealed that Co_3O_4 particles in the size of ca. 30–50 nm were highly dispersed and attached on the surface of the reticular CNF and all around. As for electrode materials, the CNF-Co_3O_4 composite demonstrated very high reversible capacity (more than 900 mAh g^{-1} in the initial 50 cycles) and excellent electrochemical cycling stability. The improved cycle performance of the CNF-Co_3O_4 composite can be attributed to its unique reticular and morphology-stable composite texture with high dispersion of Co_3O_4 nanoparticles on the CNF that provides excellent electronic and ionic conduction pathway for the electrochemical processes.

Keywords: Co_3O_4; Carbon nanofiber-Co_3O_4 composite; Anode material; Li-ion batteries

1. Introduction

Among the various sorts of transition metal oxides, spinel Co_3O_4 is an important magnetic p-type semiconductor, which has been widely used in many fields, such as solid-state sensors, supercapacitors, heterogeneous catalysts, and electrochromic devices [1–3]. Such a broad perspective of utilization makes the preparation of nanostructural Co_3O_4 much more attractive [4,5]. So far, Co_3O_4 and some other transition metal oxides have been reported to have high capacity for advanced lithium batteries [6–9]. But the Co_3O_4 active material, in general, undergoes a large irreversible capacity loss (ca. 32%) in the 1st cycle and relatively fast capacity fading rate during electrochemical cycling. On the other hand, carbon nanofibers and carbon nanotubes have been used as a promising supporting material in both heterogeneous catalysis and electrocatalysis because of their unique properties, such as high external surface, good electronic conductivity, and high mechanical stability [10–12]. Due to high specific capacity, low electrode potential, high columbic efficiency, long cycle life and a high level of safety, several types of carbon nanofibers have been successfully used in lithium battery applications [13,14].

In this work, a new CNF-supported cobalt oxide composite anode material was prepared by the precipitation of $Co(OH)_2$ on the surface-activated CNF and subsequent calcination in argon flow. In rechargeable lithium batteries, this new composite material shows very high reversible Li-storage capacity and excellent electrochemical cycling stability. It could be a promising anode material for advanced Li-ion batteries.

2. Experimental

The commercial carbon nanofiber with average diameter of 200 nm was pretreated in concentrated HNO_3–H_2SO_4 (4:1, v/v) solution at 85 °C for 5 h, intensively washed with deionized water and dried in vacuum. A given amount of $Co(NO_3)_2{\cdot}6H_2O$ was dissolved into 100 ml of isopropyl alcohol–water (1:1, v/v) solution in a three-necked round-bottom. 0.2 g of acid-treated CNF was dispersed in the above solution by ultrasonication for 0.5 h and then stirred for several hours under an argon flow. Then appropriate amount of isopropyl alcohol–ammonia solution was added into the suspending solution and aged for hours to ensure complete precipitation. The CNF-$Co(OH)_2$

* Corresponding author. Tel.: +86 21 54747667; fax: +86 21 54747667.
E-mail address: Yangj723@sjtu.edu.cn (J. Yang).

0378-7753/$ – see front matter © 2007 Elsevier B.V. All rights reserved.
doi:10.1016/j.jpowsour.2007.10.073

composite precursor was obtained by filtering and drying under vacuum at 70 °C. The CNF-supported Co_3O_4 composite was finally obtained by calcining the CNF-$Co(OH)_2$ precursor at 500 °C in Ar flow for 2 h. Based on no weight loss of CNF during filtering and pyrolysis, the nominal content of CNF in the CNF-Co_3O_4 composites was calculated according to the original CNF weight (0.2 g) and the final total weight. The home-made Co_3O_4 nano-powder was prepared by the same procedures as mentioned above but without adding CNFs.

The resulting samples were analyzed by X-ray diffraction on a Rigaku diffractometer D/MAX-2200/PC equipped with Cu Kα radiation. The morphology of the samples was observed by scanning electron microscopy (SEM) on a JEOL field-emission microscope (JSM-7401F) and transmission electron microscopy (TEM) on a JEOL high-resolution electron microscope (JEM-2010). Fourier transform infrared spectroscopy was recorded on a Perkin-Elmer PARAGON 1000 FT-IR spectrometer using the potassium bromide pellet technique. Specific surface area was determined by gas adsorption on ASAP 2010 M+C (Micromeritics Inc. USA).

Electrodes were prepared by coating a slurry containing 80 wt.% active material, 10 wt.% acetylene black and 10 wt.% polyvinylidene fluoride (PVDF) binder dissolved in *N*-methyl-2-pyrrolidinone (NMP), on a copper foil and drying under vacuum at 120 °C over 3 h. A typical electrode disk contained 1.2–1.8 mg cm^{-2} active material. Electrochemical performances of the composite materials were examined via CR2016 coin cells with lithium metal counter electrode, Celgard 2700 membrane separator, and electrolyte with 1M $LiPF_6$ dissolved in the mixture of ethylene carbonate (EC) and dimethyl carbonate (DMC) (1:1, w/w). The model cells were assembled in an argon-filled glove box containing less than 1 ppm each of oxygen and moisture. Galvanostatic charge and discharge was controlled between 3 and 0.01 V versus Li^+/Li on LAND CT2001A cycler at 25 °C.

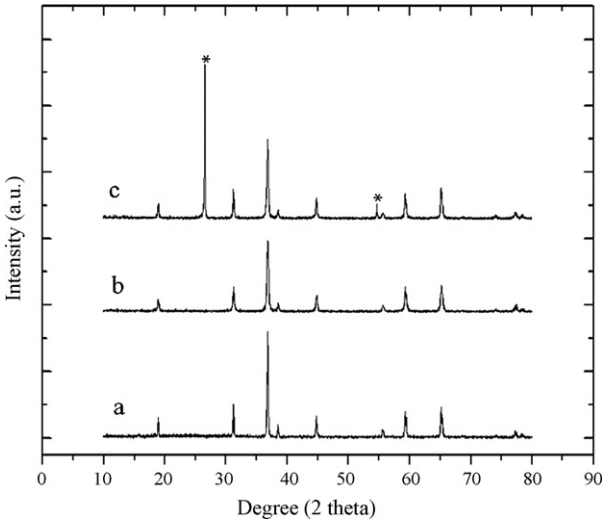

Fig. 1. X-ray diffraction patterns of commercial Co_3O_4 (a), home-made Co_3O_4 (b) and CNF-Co_3O_4 nanocomposites (c). * Response from CNF.

3. Results and discussion

The phase purity and crystallinity of Co_3O_4 samples and CNF-Co_3O_4 nanocomposite were characterized using XRD. Fig. 1 shows XRD patterns of the home-made Co_3O_4 powder and CNF-Co_3O_4 composite powder, in comparison with commercial Co_3O_4 product. The clear diffraction peaks of all the samples represent a typical character of the crystalline face-centered cubic (fcc) Co_3O_4 phase [space group: $Fd\bar{3}m$ (2 2 7)]. The (3 1 1) reflection of Co_3O_4 of the synthesized samples was used to calculate the average grain size according to the Scherrer formula. The average grain size of home-made Co_3O_4 and CNF-Co_3O_4 composite was ca. 27.5 and 30.9 nm, respectively.

Fig. 2 exhibits SEM images of commercial Co_3O_4, home-made Co_3O_4, acid-treated CNF and the CNF-Co_3O_4 composite. Commercial Co_3O_4 powder has two particle size distributions, mainly at ca. 500–1000 nm and in small part at ca. 100 nm. The

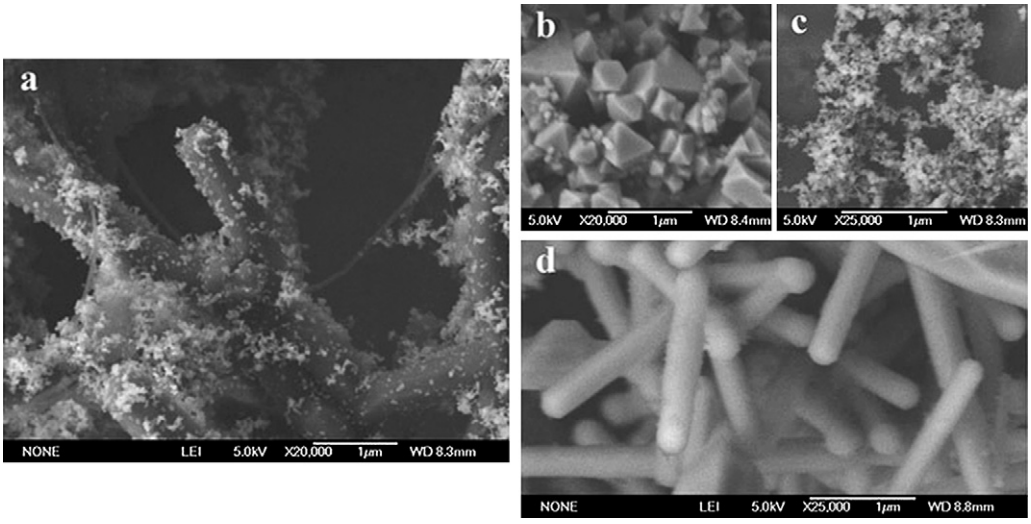

Fig. 2. FE-SEM images of CNF-Co_3O_4 nanocomposite with 16.7 wt.% CNF (a), commercial Co_3O_4 (b), home-made Co_3O_4 (c) and acid-treated CNF (d).

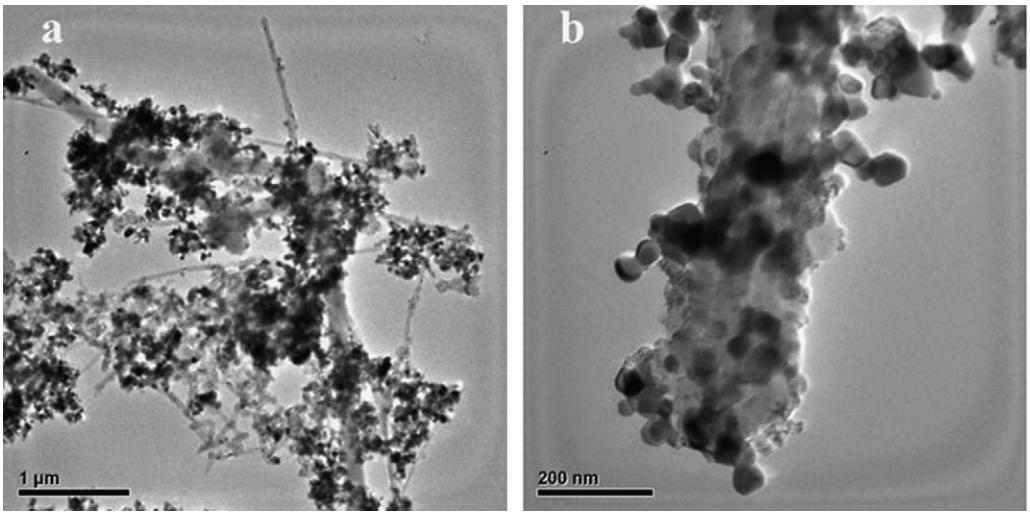

Fig. 3. TEM images of CNF-Co_3O_4 nanocomposites with 16.7 wt.% CNF.

home-made Co_3O_4 powder presents a more uniform particle distribution with the particle size of ca. 30–50 nm. For CNF-Co_3O_4 composite, Co_3O_4 nanoparticles are homogenously dispersed on the surface of CNF and all around (Fig. 2a). The CNF substrate used here has fiber diameters from ca. 50 to 300 nm with an average of 200 nm. Fig. 3a shows typical TEM image of the CNF-Co_3O_4 composite. The pristine CNFs have the lengths ranging from several to tens of micrometers and form a closely connected network via entangled and branched CNF. The fine dispersion and tight attachment of the Co_3O_4 nanoparticles in size ranged from 30 to 50 nm on the individual CNF is observable from Fig. 3b.

After oxidative pretreatment with nitric acid, a great deal of functional carboxyl groups can be formed on the surface of CNF [15,16]. As a result, the surface of the CNF becomes more hydrophilic. Due to a strong binding affinity of cobalt ions to the carboxyl groups, cobalt ions will be trapped near the surface of CNF, as in the case of virus [9]. When the ammonia solution is added into the above solution under an argon flow, cobalt ions, trapped near the CNF surface and dispersed in the solution, will be converted into α-$Co(OH)_2$ deposit, which has been confirmed by XRD measurement, and the CNF-$Co(OH)_2$ composite precursor is formed. Finally the CNF-Co_3O_4 composite is obtained by the calcination of the CNF-$Co(OH)_2$ precursor at 500 °C in Ar flow.

The electrochemical performance of the commercial Co_3O_4, home-made Co_3O_4 nano-powder and the CNF-Co_3O_4 composite was investigated and compared. Fig. 4a exhibits the discharge (lithiation) and charge (delithiation) profiles for the CNF-Co_3O_4 composite electrode containing 16.7 wt.% CNF. The voltage trend is well indicative of typical characteristics of Co_3O_4 electrode, that is, a long voltage plateau at about 1.07 V followed by a sloping curve down to the cut-off voltage of 0.01 V during the first discharge step. According to the investigations by groups of Thackeray and Tarascon [17,18], the voltage plateau at 1.07 V is related to a conversion from Co_3O_4 to an intermediate phase ($Li_xCo_3O_4$ or CoO), and then to Co, whereas the sloping portion

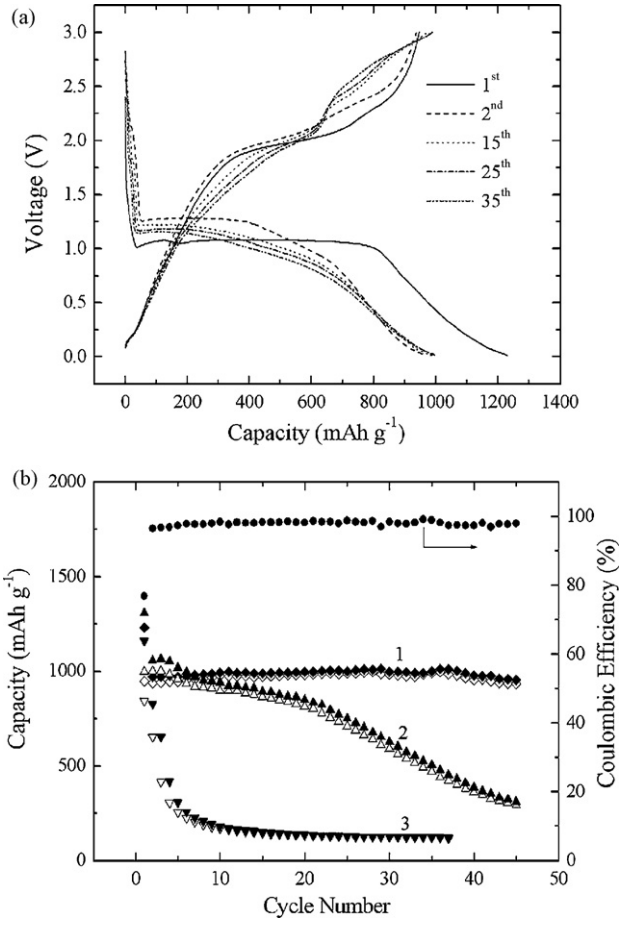

Fig. 4. (a) Typical charge and discharge profiles of CNF-Co_3O_4 nanocomposite and (b) capacity-cycle number curves of different samples and coulombic efficiency of CNF-Co_3O_4 composite during cycling, (1) CNF-Co_3O_4 nanocomposite, (2) home-made Co_3O_4, (3) commercial Co_3O_4, solid and hollow point symbols represent lithium insertion and extraction, respectively, cycling was controlled between 0.01 and 3.0 V vs. Li/Li^+ at a current rate of 100 mA g^{-1}.

down to 0.01 V is predominantly associated with the formation of a polymer/gel-like film [19,20], which disappears in the following charge process but the electrochemical reversibility is maintainable during cycling. For the charge process, the reverse electrochemical reactions, against the above discharge ones, take place. Ex situ X-ray diffraction reveals that the diffraction peaks of cobalt oxide almost disappear after full lithiation. According to the literature [6,19], amorphous Li_2O and nanosized Co products are formed. Moreover, original XRD peaks of Co_3O_4 phase can be hardly detected for a completely delithiated sample. It means that the crystalline cobalt oxide is converted to amorphous one after electrochemical cycling.

The first reversible capacity concerning lithium extraction is about 946.8 mAh g^{-1} for CNF-Co_3O_4 composite. In view of the fact that CNF has a stable delithiation capacity of ca. 300 mAh g^{-1}, the contribution of Co_3O_4 to the total capacity is about 1078 mAh g^{-1}, larger than its theoretical one (890 mAh g^{-1}). The extra capacity may result from the above-mentioned formation/dissolution of the polymer/gel-like film as well as much larger effective surface and grain boundary area of the nanosized Co_3O_4 particles, which may offer extra sites for Li ions. The BET surface area of CNF-Co_3O_4 composite powder is 22.12 m^2 g^{-1}, which is about 8 times larger than that of commercial Co_3O_4. On the other hand, a capacity loss of about 23% is observed in the first cycle due to the formation of partial irreversible solid electrolyte interface (SEI) film and the microstructural changes in the active material and in the electrode. The coulombic efficiency rapidly rises from 77% in the 1st cycle to 97% in the 2nd one, and then an efficiency of mostly above 98% maintains in the following cycles (see Fig. 4b). Even after 100 cycles, the reversible capacity of CNF-Co_3O_4 composite is still kept at 776.3 mAh g^{-1} and much higher than that of graphite (372 mAh g^{-1}), which is about 82% of the initial value. With an increase of CNF amount in the composite, the capacity regularly declines, but the long-term rechargeability is further improved.

In contrast, a drastic difference in the cycling behavior is observed for the active materials without CNF support. Even though the first Li-extraction capacities of the commercial and home-made Co_3O_4 electrodes are 843 and 997 mAh g^{-1}, further cycling leads to a rapid decay of the capacity to 122 and 515 mAh g^{-1}, respectively after 35 cycles shown in Fig. 4b. A similar result was obtained by Wang et al. for a nanocrystalline Co_3O_4 electrode [21].

The excellent electrochemical activation and reversibility of CNF-Co_3O_4 nanocomposite can be attributed to its unique texture and structure. First, it is well known that nanomaterials can improve the rate capabilities of solid-state electrodes used in batteries due to substantial advantages concerning mass and charge transport by shorten effective diffusion lengths for both electronic and ionic transport [22,23]. In addition, with decreasing particle size, an increasing proportion of the total number of atoms lies on the surface, making the structural strains more and more active for the electrochemical reaction. Second, the reticular CNF-Co_3O_4 nanocomposite structure of entangled and branched bundles of CNF can produce a higher electronic conductivity than single Co_3O_4 powder. Third, the CNF network cannot only buffer the large volume change of Co_3O_4 during the cycling process but also alleviate possible agglomeration of the finely distributed Co_3O_4 nanoparticles.

4. Conclusions

In conclusion, novel CNF-supported Co_3O_4 nanocomposite materials can be prepared by developing CNF-$Co(OH)_2$ composite precursors in aqueous solution without any surfactants and calcining the precursor under Ar flow. The reticular and morphology-stable composite texture with fine dispersion of Co_3O_4 nanoparticles on the mixed conductive CNF provides an excellent electronic and ionic conduction pathway for the electrochemical processes, which ensures high reversible capacity and excellent cycle-ability.

Acknowledgment

This work was supported by National Basic Research Program of China (973 Program, No. 2007CB209705).

References

[1] W.Y. Li, L.N. Xu, J. Chen, Adv. Funct. Mater. 15 (2005) 851–857.
[2] P. Nkeng, J.-F. Koening, J.-L. Gautier, P. Chartier, G. Poillerat, J. Electroanal. Chem. 402 (1996) 81–89.
[3] T. Maruyama, S. Arai, J. Electrochem. Soc. 145 (1996) 1383–1386.
[4] D. Barreca, C. Massignan, S. Daolio, M. Fabrizio, C. Piccirillo, Chem. Mater. 13 (2001) 588–593.
[5] R. Xu, H.C. Zeng, J. Phys. Chem. B 107 (2003) 926–930.
[6] P. Poizot, S. Laruelle, S. Grugeon, L. Dupont, J.-M. Tarascon, Nature 407 (2000) 496–499.
[7] Y. Yu, C.H. Chen, J.L. Shui, S. Angew. Chem. Int. Ed. 44 (2005) 7085–7089.
[8] K.T. Nam, D.W. Kim, P.J. Yoo, C.Y. Chiang, N. Meethong, P.T. Hammond, Y.M. Chiang, A.M. Belcher, Science 312 (2006) 885–888.
[9] J.S. Do, C.H. Weng, J. Power Sources 159 (2006) 323–327.
[10] C.A. Bessel, K. Laubernds, N.M. Rodriguez, R.T.K. Baker, J. Phys. Chem. B 105 (2001) 1115–1118.
[11] E.S. Steigerwalt, G.A. Deluga, C.M. Lukehart, J. Phys. Chem. B 106 (2002) 760–766.
[12] V. Hacker, E. Wallnöfer, W. Baumgartner, T. Schaffer, J.O. Besenhard, H. Schröttner, M. Schmied, Electrochem. Commun. 7 (2005) 377–382.
[13] K. Suzuki, T. Iijima, M. Wakihara, Electrochim. Acta 44 (1999) 2185–2191.
[14] J.K. Lee, K.W. An, J.B. Jub, B.W. Cho, W.I. Cho, D. Park, K.S. Yun, Carbon 39 (2001) 1299–1305.
[15] S.C. Tsang, Y.K. Chen, J.P.F. Harris, M.L.H. Green, Nature 372 (1994) 159–162.
[16] Z. Wu, C.U. Pittman, S.D. Gardner, Carbon 33 (1995) 597–605.
[17] M.M. Thackeray, S.D. Baker, K.T. Adendorff, J.B. Goodenough, Solid State Ionics 17 (1985) 175–181.
[18] D. Larcher, G. Sudant, J.B. Leriche, Y. Chabre, J.M. Tarascon, J. Electrochem. Soc. 149 (2002) A234–A241.
[19] S. Laruelle, S. Grugeon, P. Poizot, M. Dollé, L. Dupont, J.-M. Tarascon, J. Electrochem. Soc. 149 (2002) A627–A634.
[20] M. Dollé, P. Poizot, L. Dupont, J.-M. Tarascon, Electrochem. Solid State Lett. 5 (2002) A18–A21.
[21] G.X. Wang, Y. Chen, K. Konstantinov, M. Lindsay, H.K. Liu, S.X. Dou, J. Power Sources 109 (2002) 142–147.
[22] A.S. Arico, P.G. Bruce, B. Scrosati, J.M. Tarascon, W.V. Schalkwijk, Nat. Mater. 4 (2005) 366–376.
[23] J. Maier, Nat. Mater. 4 (2005) 805–815.